THE JOURNAL OF PHYSICAL CHEMISTRY C

Article

pubs.acs.org/JPCC

Ultrafast Carrier Dynamics in Hematite Films: The Role of Photoexcited Electrons in the Transient Optical Response

Shayne Sorenson, Eric Driscoll, Shima Haghighat, and Jahan M. Dawlaty*

Department of Chemistry, University of Southern California, Los Angeles, California 90089, United States

S Supporting Information

ABSTRACT: Hematite (Fe_2O_3) is a promising earth-abundant, visible light absorber, and easily processable photocatalytic material. Understanding the dynamics of photogenerated electrons and holes in hematite and their optical signatures is crucial in designing hematite thin film devices such as photoanodes for water oxidation. We report carrier dynamics in hematite films as measured by ultrafast transient absorption spectroscopy (TA) with a pump pulse centered at 400 nm (3.1 eV) and a probe pulse spanning the visible range. We observe a small negative response for wavelengths shorter than 530 nm (2.34 eV) and a large positive response for longer wavelengths. We interpret the spectrally resolved TA data based on recent electronic band structure calculations, while accounting for excited state absorption, ground state bleach, and stimulated emission within the relevant bands. We propose that the origin of the positive TA response is absorption of the probe by photoexcited electrons within the conduction bands. This interpretation is consistent with features observed in the data, specifically an abrupt boundary near 530 nm, a diffuse edge at lower energy probes with a ~ 250 fs decay time characteristic of carrier relaxation, and slower decay components of ~5.7 and >670 ps characteristic of carrier recombination. We propose that the negative TA signal arises at short wavelengths where excited state absorption within the conduction bands is no longer possible and ground state bleach and stimulated emission dominate. This study will assist in understanding the origins of transient optical responses and their interpretation in hematite-based devices such as photoanodes.

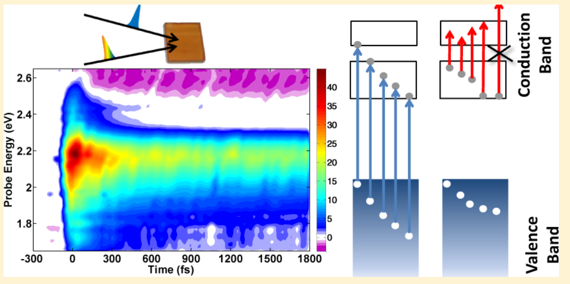

INTRODUCTION

Iron oxides have widespread relevance to many areas of science and technology.[1] Recently, there has been a renewed interest in iron oxides for their potential as light harvesting materials.[2] Their low cost, abundance, processability, optical absorption, and minimal environmental foot-print makes oxides of iron a promising candidate. In particular, hematite (Fe_2O_3), has shown a potential for water oxidation, which is the more kinetically challenging half-reaction of many solar-to-fuel proposed routes.[3,4]

Understanding the electronically excited states of hematite is essential to its application in light harvesting devices, particularly as a photocatalyst. Although the structure of hematite has been known for a long time,[5] its electronic structure, particularly that of its excited states, still remains an active area of study. Modern tools of computational chemistry have been used to study the electronic structure of hematite.[6−18] The bandgap of hematite varies between 1.9 to 2.2 eV and is dependent on the method of preparation, extent of crystallinity, and structure at the nanoscale.[2,19] The valence band of hematite is composed of oxygen 2p and iron 3d type orbitals. The two conduction bands of hematite are primarily of iron 3d character, with the t_{2g} and e_g type orbitals corresponding to the lower and upper conduction bands, respectively.

Studies of excited state dynamics of single crystal, thin films, and nanostructured hematite have been reported.[19−29] While the methods of preparation, dopants, and the details of the experiments vary, some observed transient absorption (TA) features are common. Upon photoexcitation of hematite above the bandgap, with a UV−visible pulse, transient absorption of hematite is enhanced (positive signal) for probe energies significantly below the band gap, while a bleach (negative TA) is observed for higher energies. While these features are common, interpretations vary and a consensus on their assignment has not been reached. The positive signal has been attributed to either absorption within the valence band into photogenerated holes[22] or absorption of electrons in trap states.[30,31] The negative signal is attributed to absorption into impurity states in the conduction band edge.[22] The observed TA signals usually show multiple decay times[20,30,32] that are interpreted as intraband relaxation of carriers (<1 ps) and interband carrier recombination (in excess of 100 ps).[20,28,30,33] The observed long decay times of the TA signal increase further as anodic (positive) potential is increased in hematite photoanode in contact with an electrolyte.[22,25]

Received: August 15, 2014
Revised: September 23, 2014
Published: September 23, 2014

dx.doi.org/10.1021/jp508273f | J. Phys. Chem. C 2014, 118, 23621−23626

In this work, we report on the ultrafast relaxation of carriers in hematite films measured by transient absorption spectroscopy. The films were prepared on sapphire using the photochemical metal organic deposition (PMOD) technique. Similar films deposited on fluorine-doped tin oxide (FTO) have been used for electrochemical water oxidation in our laboratory. We have chosen a sapphire substrate for its wide band gap, ensuring minimal influence on the measured TA signal. We report the transient optical response of the hematite film after optical excitation above the bandgap. Our interpretation of the TA signal has two distinguishing features. First, we interpret our data in light of the calculated bandstructure of hematite, including both of the conduction bands which have a dominant iron 3d character. Second, as is necessary for all TA experiments, we consider all possible optical interactions of the probe (ground state bleach, excited state absorption, and stimulated emission) in the interpretation of the signal. Our data suggests that the TA signal is dominated by absorption of photoexcited electrons within the conduction band for lower energy probes, while high energy probes experience reduced absorption due to ground state bleach and stimulated emission. This work will contribute to interpreting optical experiments on iron oxide and related materials, bringing them closer to photoelectrochemical applications.

■ EXPERIMENTAL SECTION

Iron oxide thin films were prepared using the PMOD technique,[34] which yields poly crystalline films. This method has been used previously to prepare films on fluorine doped tin oxide (FTO) for electrochemical studies.[35] In this method, a photosensitive precursor solution is spin-coated onto a substrate and then exposed to UV radiation. A 15% w/w solution of iron(III)ethylhexanoate (50% in mineral spirits, Alfa Aesar) in hexane was prepared using 0.058 g of Iron(III)-ethylhexanoate and 0.142 g of hexane. Sapphire substrates (MTI Corp.), of 0.5 mm thickness, were cleaned ultrasonically in ethanol followed by acetone then dried under air streaming. A few drops of the solution were dispensed onto the substrate by spin coating at a rate of 3000 rpm for 1 min. The film was then irradiated under a UV lamp (254 nm) until removal of organic ligands was complete, leaving an amorphous metal oxide film on the substrate. The thin film was annealed at T = 600 °C for 1 h in air using a Vulcan A-550 oven. The film was characterized by X-ray diffraction (XRD) and energy dispersive X-ray spectroscopy (EDX), as shown in the Supporting Information. The film thickness, measured by profilometry, was determined to be ~150 nm. The steady state absorption spectrum of a typical thin film is shown in Figure 1. Film thickness could be increased by performing the spin coating step multiple times prior to annealing. The films used in the transient absorption spectroscopy experiments were 5 layers thick.

A frequency resolved transient absorption apparatus was used to measure the transient response of the film upon optical pumping with a short pulse. The probe pulses were prepared by focusing 0.30 (±0.02) mW of the output of a 1 kHz regenerative amplified Ti:sapphire laser onto a 3.0 mm thick sapphire plate, resulting in white light covering most of the visible range. The pump pulses were prepared either from the second harmonic of the 800 nm or from a tunable optical parametric amplifier (OPA) system. The pump pulse was modulated at 500 Hz by an optical chopper (Thorlabs), and spectra were collected for every probe shot on a CCD camera

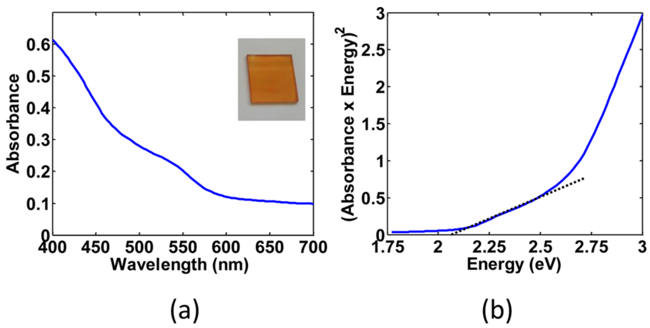

Figure 1. (a) Steady state absorption spectrum of a typical hematite film showing its characteristic red color. (b) Tauc plot[36,37] for hematite absorption (with the direct band gap and parabolic bands assumptions) pointing to a band gap of 2.1 eV, typical of hematite films.[2]

(Horiba). The transient absorption was calculated at each wavelength using two temporally adjacent probe shots. Assuming negligible power fluctuations between adjacent shots, this scheme yields results that are insensitive to power drift. The minimum detectable transient signal was determined to be 0.5 mOD by measuring the noise at negative pump−probe delays. The typical diameter of the focus spot size was ~180 (±30) μm for the pump and ~150 (±30) μm for the probe.

To obtain the chirp of the probe pulse, cross correlation of the pump and probe pulses was measured by replacing the sample with sapphire. The pump−probe data were corrected to account for this chirp. The width of the spectrally resolved cross correlation was about 200 fs for each spectral component of the probe, which is representative of our experimental time resolution. We consistently observed transient absorption at positive delays much longer than the pulse overlap from bare conventional microscope slides, and even quartz, which likely arose from the response of the impurities and multiphoton band-to-band transitions in silica. This prompted us to use sapphire, which is a large band gap material, as a substrate for the preparation of the iron oxide film. Bare sapphire substrates did not show any long-time transient signal, even in conditions of large pump power. We hope this point is taken into account in transient optical studies of thin films of hematite and other catalysts on transparent electrode substrates.

It should be emphasized that transient absorption measurements in the typical geometry, can only measure transient transmission. As such, if the pump causes enhanced reflection of the probe, it can be misinterpreted as enhanced absorption. For that reason, we also measured the transient reflection from the sample and verified that it is negative (i.e., reduced reflection). Thus, the positive measured values in the transmission geometry are truly due to enhanced absorption in the sample and not due to enhanced transient reflection.

■ RESULTS

We begin by presenting the frequency resolved transient absorption data and pointing out the significant observed features. Then we interpret the results in light of the electronic band structure of hematite. A typical frequency resolved transient absorption signal of the hematite film obtained with a pump fluence of 1.15 (±0.01) mJ/cm^2 is shown in Figure 2. We identify two separate time-scales in the data: a fast, broad-band and positive response up to ~250 fs followed by a slower

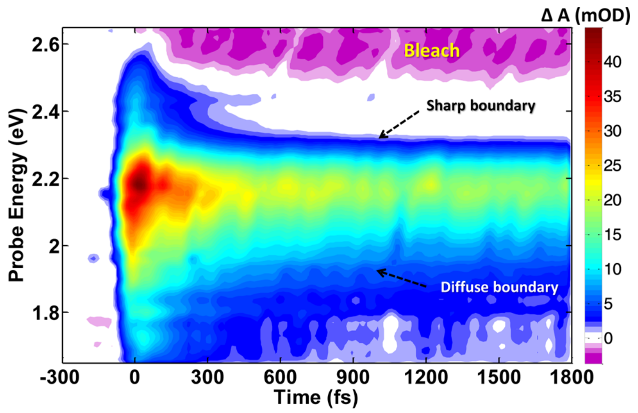

Figure 2. Typical transient absorption (TA) signal for hematite, pumped with a pulse centered at 400 nm (3.1 eV) and probed in the visible range. The positive TA signal shows a sharp boundary near 530 nm (2.34 eV) and a diffuse boundary at smaller probe energies. At higher probe energies, negative TA dominates the signal. These features are interpreted in the text.

response extending to many hundreds of picoseconds. The short-time response shows enhanced transient absorption in the range of 1.65−2.45 eV (750−506 nm) and reduced transient absorption (bleach) in the range of 2.5−2.65 eV (496−468 nm). The long-time response is postive in the 2.0−2.3 eV (620−540 nm) range. In both time ranges the magnitude of the bleach is relatively small compared to the maximum of the enhanced absorption. We have obtained scans extending to 680 ps (Figure 3) and have identified a slow decay

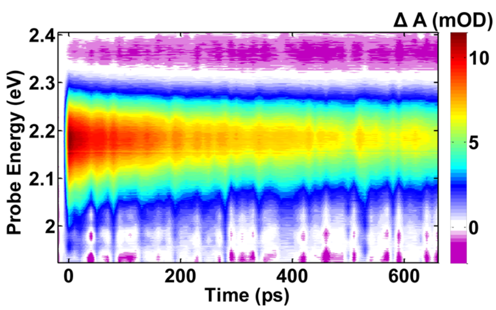

Figure 3. Transient absorption (TA) of hematite for extended probe delays. The slow decay of the positive signal corresponds to carrier recombination.

characterized by time constants of 5.7 and >670 ps for the 2.14 eV probe energy. The positive TA signal has a sharp boundary on the higher energy side and a diffuse boundary on the lower energy side.

We also carried out the experiment at various pump powers with the purpose of isolating potential dynamics resulting from multiple exciton interactions or higher order interaction with the pump. We did not observe a significant change in the dynamics upon changing the pump fluence from 0.15 ± 0.01 to 1.8 ± 0.01 mJ/cm^2. Figure 4 shows the transient absorption signal, 5 ps after time zero, for various probe wavelengths and pump powers. The linear variation of the transient absorption signal with pump power shows that multiphoton absorption of the pump and multiple exciton interactions are not contributing to the observed signal. The decays also did not vary dramatically as pump power was changed indicating that

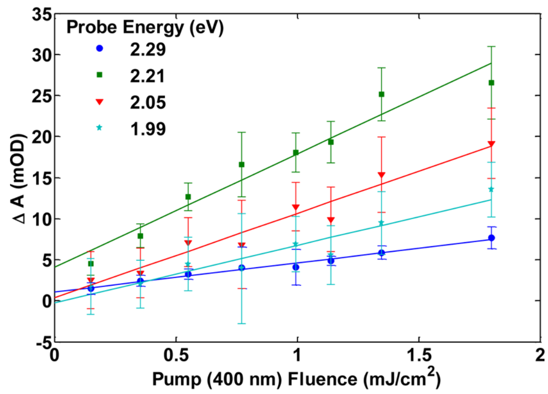

Figure 4. Dependence of transient absorption on pump fluence at a probe delay of 5 ps. Linear dependence of the TA signal on pump power demonstrates linear interaction of the pump with the sample.

higher order kinetics do not play a significant role in the material response at these powers.

■ DISCUSSION

Relating transient optical response to carrier dynamics is only possible if contributions from all relevant optical processes are accounted for. As is well-known, the measured transient absorption of the probe is a sum of at least three contributions, excited state absorption, ground state bleach, and stimulated emission. For that reason, to interpret the transient absorption data, we refer to the calculated electronic structure of hematite in recent literature[6−18] for guidance. The reported calculated DOS for the conduction bands are qualitatively consistent in the literature, with small variations in bandwidths and separation between conduction bands. As will be shown below, our analysis of the transient absorption of hematite can provide a point of reference for theorists to compare their calculated DOS for conduction bands with experimental results. A typical calculated projected density of states for hematite adapted from ref 8 is shown in Figure 5a. The valence band of hematite is composed of O 2p and Fe 3d type orbitals. The two conduction bands of hematite are primarily of Fe 3d character, with the t_{2g} and e_g type orbitals corresponding to the lower and upper conduction bands. The calculated bandgap is ∼1.9 eV, and the Fermi level lies in the bandgap. The combined width of the conduction bands, which we define as the energy difference between the bottom of the lower conduction band and the top of the upper conduction band, is also ∼1.9 eV.

Figure 5b,c summarizes the interactions of the pump and the probe with hematite in transient absorption spectroscopy. To facilitate visualization, the widths of the conduction bands, the band gap, and the arrows representing optical interactions in the diagrams are drawn to scale. First, a 400 nm (3.1 eV) pump pulse with a fwhm bandwidth of 6.0 nm (0.047 eV) generates a range of electrons and holes. Thus, the pump populates the first conduction band and the bottom edge of the second conduction band. After the pump, the photoexcited carriers begin to relax as the white-light probe pulse interacts with the sample. We examined only the visible components of the probe from 470 to 750 nm (2.64 to 1.65 eV). The possible interactions of the probe are shown in Figure 5c and include stimulated emission (SE), ground state bleach (GB), excited electron absorption (EA), and excited hole absorption (HA) i.e. ”hole-filling”. Clearly the contributions of these processes to the optical absorption spectrum must have different signs. The EA

dx.doi.org/10.1021/jp508273f | J. Phys. Chem. C 2014, 118, 23621−23626

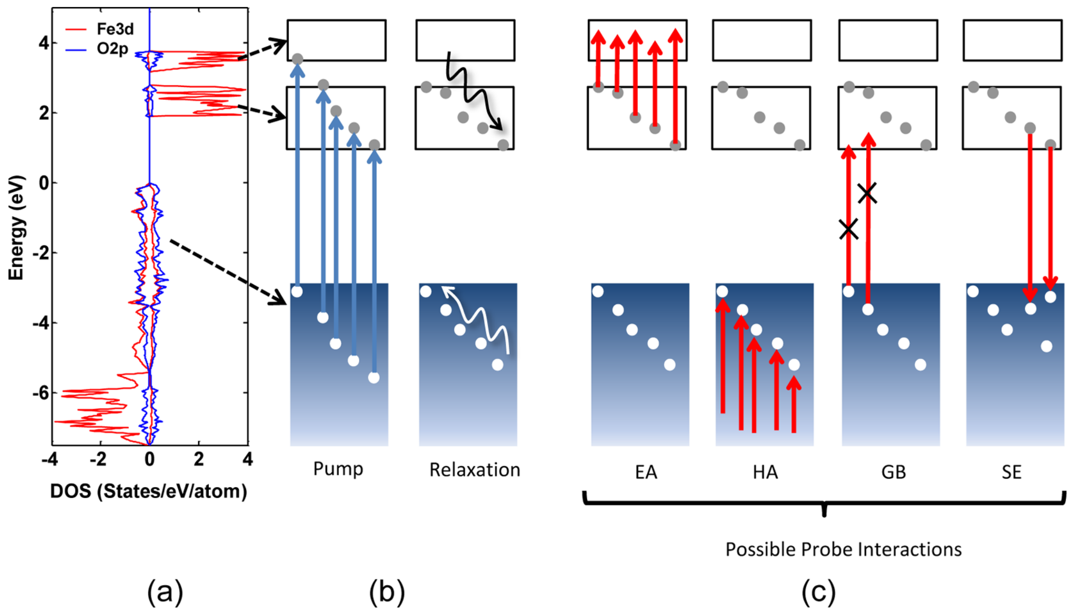

Figure 5. (a) Calculated density of states of hematite adapted from ref 8. The valence band has mixed character of oxygen 2p and Fe 3d orbitals. The two conduction bands are composed of t_{2g} and e_g type orbitals. (b) Optical excitation with 3.1 eV pump, as used in the experimental work, generates a range of holes and electrons within the conduction and valence bands, which consequently relax to the band edges. (c) The probe can interact with the photoexcited holes and electrons in many ways. In the excited state electron absorption (EA) process the probe promotes intraband transitions in the conduction band. In the excited state hole absorption (HA) process the photogenerated holes are filled via intraband transitions in the valence band. Ground state bleach (GB) corresponds to the reduced absorption of the probe due to the photogenerated holes. Stimulated emission (SE) is the downward transition from the conduction to the valence band. Out of these processes, EA and HA result in enhanced absorption (positive TA signal) and GB and SE result in reduced absorption (negative TA signal) for the probe. The total transient absorption signal is determined by the relative transition dipole moment and joint-density of states of these transitions. Our data suggests that EA is the dominant process in the transient absorption of hematite for probe energies less than 2.3 eV.

and HA processes result in enhanced absorption (positive TA signal), while SE and GB result in reduced absorption (negative TA signal). The overall TA signal at a given wavelength arises from the sum of all these contributions.

According to a basic model of band-to-band optical transitions (Fermi's golden rule), at least three factors determine the strength of these optical interactions. The first factor, the joint density of states, is the product of the density of states between the initial and final states in a transition. The second factor is the strength of the transition dipole moment that couples an initial and a final state. The third factor is the difference in occupancy between the initial and final states (i.e., if the final and initial states have equal occupancy, the upward and downward transitions are equally probable, resulting in no net absorption).

Using this model, we return to the experimental data in Figure 2 and begin by pointing out that in positive regions HA and EA must dominate. We further propose that the positive signal arises mostly from EA rather than HA. This is supported by the sharp boundary near 2.3 eV, above which the signal is no longer positive, and the diffuse boundary for lower energy probes. We demonstrate in Figure 6 that the EA process must not be possible for probe energies that exceed the combined width of the conduction bands. Thus, at energies higher than the combined width of the conduction bands, the EA process no longer dominates the negatively contributing GB and SE processes and a change of sign in the signal (i.e., boundary) must be observed. We propose that the HA process is unlikely to cause such a spectral boundary because the valence band is much wider (>5 eV) than the highest energy of our probe pulse and of uniform character (O 2p and Fe 3d hybrid character).

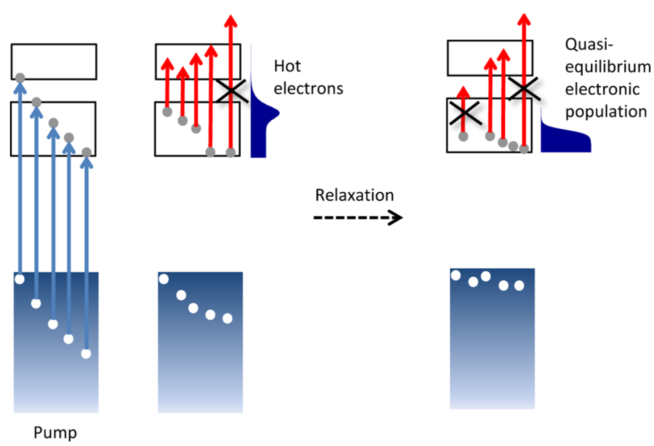

Figure 6. Energy dependence of the excited state electron absorption (EA). Probes with energy higher than the combined width of the two conduction bands can not cause EA, allowing the bleach signals to dominate. This is manifested as the sharp boundary near 2.3 eV in our observed data (Figure 2). Initially (<250 fs) low energy probes can cause EA of the photoexcited hot electrons with the highest energy. However, as relaxation progresses, low energy probes are gradually unable to cause EA. This is evident in the diffuse boundary in our observed TA data (Figure 2) corresponding to electron relaxation in the conduction band.

Thus, valence-to-valence transitions would have a relatively uniform magnitude over the spectral range of the probe. Furthermore, the joint density of states (JDOS) for the valence-to-valence transitions is much smaller than that of the conduction-to-conduction band transitions as can be inferred from Figure 5.a, reducing the contribution of HA compared to

EA to the positive signal. Using 3 states/eV/atom as a rough estimate for the average DOS of the conduction bands and 1 state/eV/atom throughout the valence band results in a JDOS for conduction-to-conduction transitions that is greater than that of valence-to-valence transitions by a factor of 9. Finally the valence-to-valence optical transitions are likely to have small transition dipole moments, both due to the localized nature of the initial and final states and the similarity of orbital types between them. In contrast, it has been argued[38] that the transitions between the two conduction bands are more delocalized and involve transfer of electrons between two neighboring metal atoms. Such transitions are expected to have large transition dipole moments and not follow the strict symmetry rules of forbidden transitions between d-orbitals. Thus, we identify EA as the dominant source of the positive transient absorption signal. Based on this, the sharp edge at 2.3 eV revealed in our measurement corresponds to the combined width of the two conduction bands. This value is useful both for theoreticians as a benchmark in calculating the electronic structure of the excited states and for experimentalists involved in measuring excited state dynamics of hematite. We emphasize, once again, that SE and GB only result in negative contribution to TA. Thus, the observed maximum of the positive signal, although near the bandgap energy, can not be due to SE and GB and as argued here, is due to EA.

With the EA process as the dominant cause of the positive signal, the diffuse edge of the TA signal at lower probe energies can also be explained. This edge arises from the EA process from the high energy tail of the distribution of photoexcited electrons in the conduction band. This is supported by the fact that immediately after absorption of the pump, when the photoexcited electron population is out of equilibrium, transitions as low as 1.7 eV are permitted from the high energy tail of this hot population to the second conduction band. As the electrons relax within the lower conduction band, the energy necessary to excite the hottest electrons to the next excited state increases. This dynamic is captured in the continuous increase in energy of the transient absorption diffuse edge (Figure 1) with a time constant of ∼250 fs. This time constant represents relaxation of hot electrons within the lower conduction band and lies reasonably well within the range expected for typical semiconductors and is in agreement with previous measurements on hematite.[2,20] Once the carriers have fully relaxed in the lower conduction band, they still undergo EA, and the signal beyond 1 ps is due to EA from this relaxed population. The recombination of the relaxed electrons with holes is captured in the slower components (5.7 and >670 ps; Figure 3).

The results reported here agree with previous experiments performed on various forms of hematite.[19−26] Common features include positive TA signals below the bandgap energy, negative signal well above the bandgap energy, and decay times comparable to those reported here. Despite all these works, a consensus has yet to be reached on the origins of the observed features. Some works attribute the positive signal to hole absorption,[22−24] while others attribute it to absorption by trapped electrons.[20] As it stands there is a great need to unify our understanding of how the various optical processes due to both electrons and holes contribute to the TA spectrum of hematite. For the first time, we have interpreted the TA signal of hematite in light of the recently calculated DOS of hematite, accounting for all possible probe interactions and their relative strengths. We conclude that a consistent explanation of the TA signal in various spectral regions requires that the excited EA process be dominant over HA. Furthermore, our interpretation identifies the maximum absorption energy of what is often referred to as trapped electrons, and places their relative energy level close to the bottom of the conduction band.

Including the EA process in the interpretation of TA signals will enhance our understanding of the excited state dynamics in hematite. Consideration of EA is specifically relevant for hematite photoanodes in contact with electrolyte, where many chemical and charge transfer processes also occur, complicating the interpretation of TA experiments. The positive sign of the transient absorption of hematite has been ascribed to hole dynamics, based on evidence from potential dependence studies.[22] Our work provides evidence that excited electron absorption (EA) has a stronger contribution to the positive signal, at least within our experimental time-scale. Theoretical input, in particular detailed calculations of optical absorption strengths between various bands and their combined contribution to the optical response, will be valuable in relating spectroscopic observations to carrier dynamics. We hope that future concerted efforts in interfacial spectroscopy, electronic structure theory, and electrochemistry shed further light on the excited state dynamics of hematite−electrolyte junctions.

■ ASSOCIATED CONTENT

Ⓢ Supporting Information

Hematite characterization data as well as further TA data is available free of charge via the Internet at http://pubs.acs.org.

■ AUTHOR INFORMATION

Corresponding Author

*E-mail: dawlaty@usc.edu.

Notes

The authors declare no competing financial interest.

■ ACKNOWLEDGMENTS

The authors acknowledge support from the University of Southern California start up grant and the AFOSR YIP Award (FA9550-13-1-0128). S.S. was supported by the University of Southern California Provost Fellowship. S.H. was supported by the Mork Family Scholarship for part of the duration of this work.

■ REFERENCES

(1) Cornell, R. M. *The Iron Oxides: Structure, Properties, Reactions, Occurrences and Uses*; Wiley-VCH: Weinheim, Germany, 2003.

(2) Sivula, K.; Le Formal, F.; Grätzel, M. Solar Water Splitting: Progress using Hematite (α-Fe_2O_3) Photoelectrodes. *ChemSusChem* **2011**, *4*, 432−449.

(3) Nocera, D. G. The Artificial Leaf. *Acc. Chem. Res.* **2012**, *45*, 767−776.

(4) Tachibana, Y.; Vayssieres, L.; Durrant, J. R. Artificial Photosynthesis for Solar Water-Splitting. *Nat. Photonics* **2012**, *6*, 511−518.

(5) Pauling, L.; Hendricks, S. B. The Crystal Structures of Hematite and Corundum. *J. Am. Chem. Soc.* **1925**, *47*, 781−790.

(6) Liao, P.; Carter, E. A. Optical Excitations in Hematite (α-Fe_2O_3) via Embedded Cluster Models: A CASPT2 Study. *J. Phys. Chem. C* **2011**, *115*, 20795−20805.

(7) Liao, P.; Toroker, M. C.; Carter, E. A. Electron Transport in Pure and Doped Hematite. *Nano Lett.* **2011**, *11*, 1775−1781.

(8) Liao, P.; Carter, E. A. Testing Variations of The GW Approximation on Strongly Correlated Transition Metal Oxides: Hematite (α-Fe_2O_3) as a Benchmark. *Phys. Chem. Chem. Phys.* **2011**, *13*, 15189−15199.

(9) Liao, P.; Keith, J. A.; Carter, E. A. Water Oxidation on Pure and Doped Hematite (0001) Surfaces: Prediction of Co and Ni as Effective Dopants for Electrocatalysis. *J. Am. Chem. Soc.* **2012**, *134*, 13296−13309.
(10) Pozun, Z. D.; Henkelman, G. Hybrid Density Functional Theory Band Structure Engineering in Hematite. *J. Chem. Phys.* **2011**, *134*, 224706.
(11) Rollmann, G.; Rohrbach, A.; Entel, P.; Hafner, J. First-Principles Calculation of The Structure and Magnetic Phases of Hematite. *Phys. Rev. B* **2004**, *69*, 165107.
(12) Thimsen, E.; Biswas, S.; Lo, C. S.; Biswas, P. Predicting the Band Structure of Mixed Transition Metal Oxides: Theory and Experiment. *J. Phys. Chem. C* **2009**, *113*, 2014−2021.
(13) Wang, Y.; Lopata, K.; Chambers, S. A.; Govind, N.; Sushko, P. V. Optical Absorption and Band Gap Reduction in $(Fe_{1-x}Cr_x)_2O_3$ Solid Solutions: A First-Principles Study. *J. Phys. Chem. C* **2013**, *117*, 25504−25512.
(14) Butler, W. H.; Bandyopadhyay, a.; Srinivasan, R. Electronic and Magnetic Structure of a 1000 K Magnetic Semiconductor: α-Hematite (Ti). *J. Appl. Phys.* **2003**, *93*, 7882−7884.
(15) Rivera, R.; Pinto, H. P.; Stashans, A.; Piedra, L. Density Functional Theory Study of Al-Doped Hematite. *Phys. Scr.* **2012**, *85*, 015602.
(16) Guo, Y.; Clark, S. J.; Robertson, J. Electronic and Magnetic Properties of Ti_2O_3, Cr_2O_3, and Fe_2O_3 Calculated by The Screened Exchange Hybrid Density Functional. *J. Phys.: Condens. Matter* **2012**, *24*, 325504.
(17) Kiejna, A.; Pabisiak, T. Surface Properties of Clean and Au or Pd Covered Hematite (α-Fe_2O_3) (0001). *J. Phys.: Condens. Matter* **2012**, *24*, 095003.
(18) Nørskov, J. K.; Bligaard, T.; Rossmeisl, J.; Christensen, C. H. Towards the Computational Design of Solid Catalysts. *Nat. Chem.* **2009**, *1*, 37−46.
(19) Wheeler, D. A.; Wang, G.; Ling, Y.; Li, Y.; Zhang, J. Z. Nanostructured Hematite: Synthesis, Characterization, Charge Carrier Dynamics, and Photoelectrochemical Properties. *Energy Environ. Sci.* **2012**, *5*, 6682−6702.
(20) Joly, A. G.; Williams, J. R.; Chambers, S. a.; Xiong, G.; Hess, W. P.; Laman, D. M. Carrier Dynamics in α-Fe_2O_3 (0001) Thin Films and Single Crystals Probed by Femtosecond Transient Absorption and Reflectivity. *J. Appl. Phys.* **2006**, *99*, 053521.
(21) Zhai, T.; Yao, J. *One-Dimensional Nanostructures*; John Wiley & Sons, Inc.: Hoboken, NJ, 2013.
(22) Pendlebury, S. R.; Barroso, M.; Cowan, A. J.; Sivula, K.; Tang, J.; Grätzel, M.; Klug, D.; Durrant, J. R. Dynamics of Photogenerated Holes in Nanocrystalline α-Fe_2O_3 Electrodes for Water Oxidation Probed by Transient Absorption Spectroscopy. *Chem. Commun.* **2011**, *47*, 716−718.
(23) Barroso, M.; Pendlebury, S. R.; Cowan, A. J.; Durrant, J. R. Charge Carrier Trapping, Recombination and Transfer in Hematite (α-Fe2O3) Water Splitting Photoanodes. *Chem. Sci.* **2013**, *4*, 2724−2734.
(24) Le Formal, F.; Pendlebury, S. R.; Cornuz, M.; Tilley, S. D.; Grätzel, M.; Durrant, J. R. Back Electron-Hole Recombination in Hematite Photoanodes for Water Splitting. *J. Am. Chem. Soc.* **2014**, *136*, 2564−2574.
(25) Pendlebury, S. R.; Wang, X.; Le Formal, F.; Cornuz, M.; Kafizas, A.; Tilley, S. D.; Grätzel, M.; Durrant, J. R. Ultrafast Charge Carrier Recombination and Trapping in Hematite Photoanodes under Applied Bias. *J. Am. Chem. Soc.* **2014**, *136*, 9854−9857.
(26) Huang, Z.; Lin, Y.; Xiang, X.; Rodríguez-Córdoba, W.; McDonald, K. J.; Hagen, K. S.; Choi, K.-S.; Brunschwig, B. S.; Musaev, D. G.; Hill, C. L.; et al. In Situ Probe of Photocarrier Dynamics in Water-Splitting Hematite (α-Fe_2O_3) Electrodes. *Energy Environ. Sci.* **2012**, *5*, 8923−8926.
(27) Vura-Weis, J.; Jiang, C.-M.; Liu, C.; Gao, H.; Lucas, J. M.; de Groot, F. M. F.; Yang, P.; Alivisatos, A. P.; Leone, S. R. Femtosecond M2,3-Edge Spectroscopy of Transition-Metal Oxides: Photoinduced Oxidation State Change in α-Fe_2O_3. *J. Phys. Chem. Lett.* **2013**, *4*, 3667−3671.
(28) Xiong, G.; Joly, A. G.; Holtom, G. P.; Wang, C.; McCready, D. E.; Beck, K. M.; Hess, W. P. Excited Carrier Dynamics of α-Cr_2O_3/α-Fe_2O_3 Core-Shell Nanostructures. *J. Phys. Chem. B* **2006**, *110*, 16937−16940.
(29) Fu, L.; Wu, Z.; Ai, X.; Zhang, J.; Nie, Y.; Xie, S.; Yang, G.; Zou, B. Time-Resolved Spectroscopic Behavior of Fe_2O_3 and $ZnFe_2O_4$nanocrystals. *J. Chem. Phys.* **2004**, *120*, 3406−3413.
(30) Cherepy, N. J.; Liston, D. B.; Lovejoy, J. A.; Deng, H.; Zhang, J. Z. Ultrafast Studies of Photoexcited Electron Dynamics in γ- and α-Fe_2O_3 Semiconductor Nanoparticles. *J. Phys. Chem. B* **1998**, *102*, 770−776.
(31) Nadtochenko, V. A.; Denisov, N. N.; Gak, V. Y.; Gostev, F. E.; Titov, A. A.; Sarkisov, O. M.; Nikandrov, V. V. Femtosecond Relaxation of Photoexcited States in Nanosized Semiconductor Particles of Iron Oxides. *Russ. Chem. Bull., Int. Ed.* **2002**, *51*, 457−461.
(32) Wang, G.; Ling, Y.; Wheeler, D. a.; George, K. E. N.; Horsley, K.; Heske, C.; Zhang, J. Z.; Li, Y. Facile Synthesis of Highly Photoactive α-Fe_2O_3-Based Films for Water Oxidation. *Nano Lett.* **2011**, *11*, 3503−3509.
(33) Fan, H. M.; You, G. J.; Li, Y.; Zheng, Z.; Tan, H. R.; X, S. Z.; Tang, S. H.; Feng, Y. P. Shape-Controlled Synthesis of Single-Crystalline Fe_2O_3 Hollow Nanocrystals and Their Tunable Optical Properties. *J. Phys. Chem. C* **2009**, 9928−9935.
(34) Buono-Core, G.; Tejos, M.; Lara, J.; Aros, F.; Hill, R. Solid-state photochemistry of a Cu(II) -diketonate complex: the photochemical formation of high quality films of copper(II) oxide. *Mater. Res. Bull.* **1999**, *34*, 2333−2340.
(35) Smith, R. D. L.; Prvot, M. S.; Fagan, R. D.; Zhang, Z.; Sedach, P. A.; Siu, M. K. J.; Trudel, S.; Berlinguette, C. P. Photochemical Route for Accessing Amorphous Metal Oxide Materials for Water Oxidation Catalysis. *Science* **2013**, *340*, 60−63.
(36) Kennedy, J. H.; Frese, K. W. Photooxidation of Water at Fe_2O_3 Electrodes. *J. Electrochem. Soc.* **1978**, *125*, 709−714.
(37) Tauc, J.; Grigorovici, R.; Vancu, A. Optical Properties and Electronic Structure of Amorphous Germanium. *Phys. Status Solidi B* **1966**, *15*, 627−637.
(38) Lee, J.; Kim, M.; Noh, T. Optical Excitations of Transition-Metal Oxides under The Orbital Multiplicity Effects. *New J. Phys.* **2005**, *7*, 147.